



TITLE:

The Ion Source for the Cyclotron of Kyoto University

AUTHOR(S):

Uemura, Yoshiaki; Kokame, Jun; Yamashita, Sukeaki; Kakigi, Shigeru; Fujita, Hirokazu; Kakui, Shuzo; Maruyama, Tadahiro; Sano, Kenji; Fukuzawa, Fumio

CITATION:

Uemura, Yoshiaki ...[et al]. The Ion Source for the Cyclotron of Kyoto University. Bulletin of the Institute for Chemical Research, Kyoto University 1969, 47(2): 97-113

ISSUE DATE:

1969-03-31

URL:

<http://hdl.handle.net/2433/76277>

RIGHT:

The Ion Source for the Cyclotron of Kyoto University

Yoshiaki UEMURA*, Jun KOKAME**, Sukeaki YAMASHITA***,
Shigeru KAKIGI*, Hirokazu FUJITA*, Shuzo KAKUI****,
Tadahiro MARUYAMA*****, Kenji SANO*,
and Fumio FUKUZAWA*****

Received March 3, 1969

The mechanical design features and operating characteristics of an arc-discharge type ion source with a hot-cathode and a floating electrode are described in detail. The ion source is made of wolfram and molybdenum in parts, so that it stands arc power of 800 watts. H_2^+ ion current of 90 μA and He^{2+} ion current of 30 μA are extracted through the deflector of the cyclotron of Kyoto University. Estimation of the lifetime of a filament is made from the rate of evaporation and is in good agreement with the observed lifetime. The mechanism of ion production in this ion source is considered. The temperature-rise of the floating-electrode is found to be the most important factor for the operation of this ion source.

I. INTRODUCTION

The ion source has an important role for the performance of an accelerator. The most suitable type of ion source is different according to the type of accelerator. For a cyclotron, the ion source must be placed in a strong magnetic field and in a limited narrow space.

In the early cyclotron, ions are produced at the center of dee gap by a very simple method. A hot wolfram filament is mounted near the bottom of the vacuum chamber. Gas is fed directly into the chamber. Later modifications are to surround the filament with a hollow cone of metal and to feed gas through this cone. These modifications result in the increase of the efficiency of ionization while allowing a good vacuum in the chamber of the cyclotron, below 1×10^{-5} torr. To prevent the electron beam from bombarding the upper surface of the vacuum chamber, a hood is added over the cone. The structure of the ion source is thus replaced by a hollow cylinder closed at the top but with a hole in its side. More recent type is of a floating-electrode one, in which the hood is replaced by the insulating metal disk. This disk is charged up negatively in

* 植村 吉明, 柿木 茂, 富士田 浩一, 佐野 健治: Keage Laboratory of Nuclear Science, Institute for Chemical Research, Kyoto University, Kyoto.

** 小亀 淳: Now at Institute for Nuclear Study, University of Tokyo, Tokyo.

*** 山下 佐明: Department of Physics, Faculty of Science, Nara Women's University, Nara.

**** 角井 修三: Now at Kakui Shoten.

***** 丸山 忠博: Now at Osaka Business Office, Nippon National Cash Register Co., Ltd., Tokyo.

***** 福沢 文雄: Department of Nuclear Engineering, Faculty of Engineering, Kyoto University, Kyoto.

operation and can repel electrons backward, so that the ionizing path of primary electrons becomes longer.

In the cyclotron of Kyoto University,¹⁾ the early ion source was of a simple hood type with a canal just above the filament. Using this ion source the extracted beam of protons and deuterons was of about $90\ \mu\text{A}$, but for the alpha beam the intensity was only $3\ \mu\text{A}$ at most. Later, the floating-electrode type was developed, and sufficient increase of the intensity of alpha beam was obtained. Further, subharmonic acceleration of C^{2+} and N^{3+} ions has been made with this ion source.²⁾

In the following, for this type of ion source, the construction, performance characteristics and the mechanism of ion production are described in detail.

II. CONSTRUCTION

II-1 Body of Ion Source

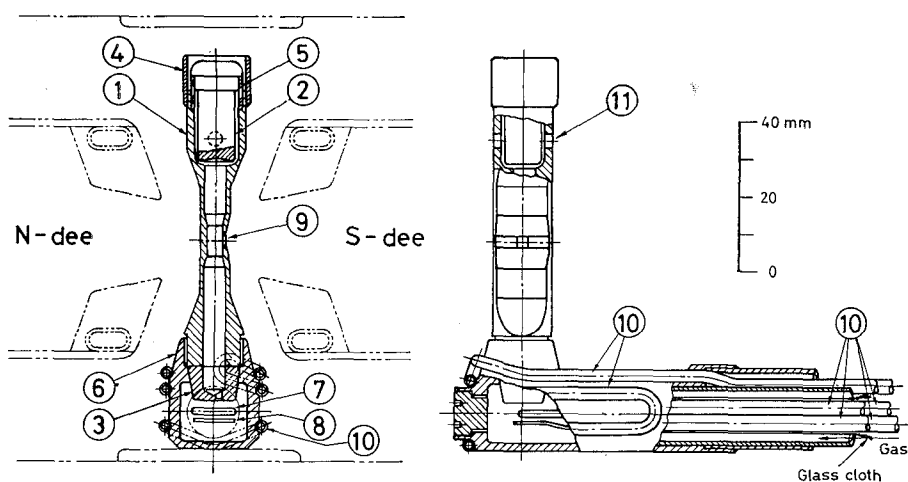


Fig. 1. Body of ion source. 1. Cavity body (Mo), 2. Repeller (W), 3. Canal electrode (W), 4. Shielding tube (Mo), 5. Insulating tube (quartz), 6. Filament chamber (Cu), 7. Filament (W), 8. Protector plate (W), 9. Aperture for ion extraction, 10. Water-cooling pipe (Cu), 11. Hole for lowering gas-pressure.

The structure of the ion source used now is shown in Fig. 1. Electrons emitted from a hot filament are accelerated by 150~300 volts and enter through a canal into the ionization cavity in which the gas pressure is of the order of 10^{-3} torr. The magnetic field of the cyclotron along the axis of the cavity confines the motion of electrons in a narrow columnar region in which many ions are produced by collisions of the electrons with gas molecules. Finally, electrons collide on the insulated electrode at the top of the cavity body and are captured in it. When the insulated electrode is charged up negatively to some extent, succeeding electrons are repelled by this electrode and go back downward continuing to ionize gas until they are captured in the cavity wall. So, the insulated electrode is called "repeller". To determine the equilibrium potential of the

repeller, in actual case, it is necessary to take into account positive ions colliding with the repeller, secondary electrons and thermal electrons from the repeller. Details of this point is described in Section V. Positive ions produced in the cavity are extracted through a hole in the side of the cavity (called "aperture for ion extraction") by the field caused by dee voltage.

The filament consists of "U"-shaped wolfram wire of 2 mm in diameter and the inside separation of the "U" is 9 mm. The filament is clamped to water-cooled copper terminals such that the "U" protrude 16 mm from the terminals. To protect the filament from being bombarded by the ions produced at the bottom of the filament-housing chamber (called "filament chamber"), a wolfram plate of 0.5 mm thick is placed beneath the filament about 1 mm apart. With this protector plate the lifetime of a filament is prolonged by a factor of two. Tantalum plate had been tried in earlier time as the protector plate. In this

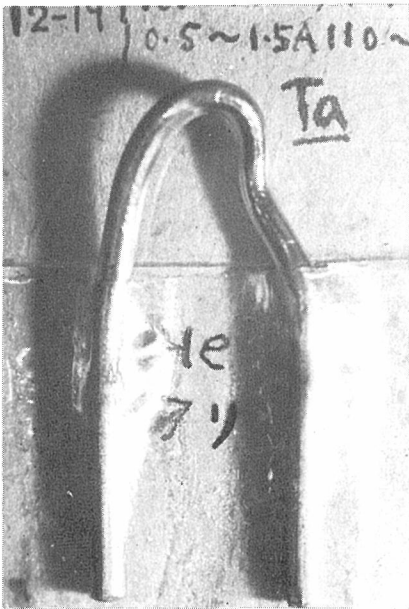


Photo. 1. Deformation of tantalum filament.

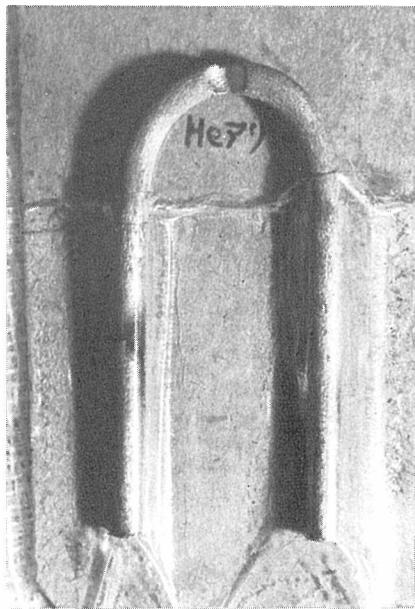


Photo. 4. Snapping of filament.

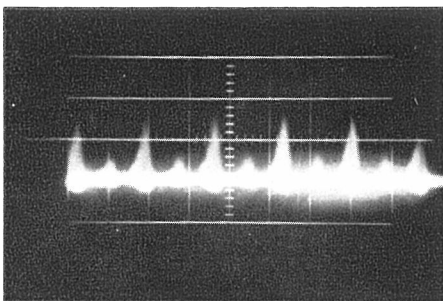


Photo. 2. 120 c/s modulation of alpha beam intensity due to ripple of arc voltage.

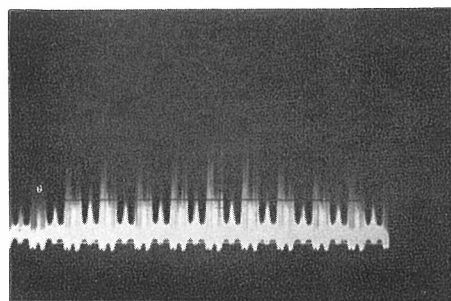


Photo. 3. 360 c/s modulation of H_2^+ ion beam intensity due to ripple of dc power of RF accelerating voltage.

case, tantalum plate was covered with wolfram evaporated from the filament after the operation of several hundred hours, and bimetallic deformation due to the change of temperature caused frequently the dead short between the filament and the protector. The filament is heated with about 200 A, dc, supplied by the selenium rectifier system described in the next section. A tantalum filament had been tried according to the recommendation of Livingston and Jones.³⁾ In our case, however, the deformation of tantalum filament due to the strong magnetic field of the cyclotron was very large. Photograph 1 shows such deformation of the tantalum filament after 18 hour operation with filament current of 160~180 A.

The filament chamber is made of copper, and water-cooling copper pipes are silver-soldered outside the chamber. A canal electrode made of wolfram is placed between the filament chamber and the ionization cavity. The canal is 2 mm in diameter in conformity with the diameter of the filament, and is 1 mm in length. This electrode is pressed in the water-cooled filament chamber with a taper of 2.5/10 by the cavity body.

The wolfram repeller is supported by an insulating quartz tube on the top of the cavity body. The surface area of the repeller is 12 cm². The insulating tube is of 12.0 mm in inner diameter and of 4.0 mm in effective insulating length. The quartz insulator is shielded by a molybdenum tube as shown in Fig. 1. In early stage, a cap-type copper shield had been tried with the result that the upper part of it had been melted shortly with arc power of 600 watts. Present molybdenum tube type can stand the arc power as large as 800 watts. The cavity body is fastened to the filament chamber by screw coupling. The cavity body is made from a molybdenum rod of 16 mm in diameter and of 74 mm in height, and the middle part has a flat-shape of 8 mm thick over the length of 35 mm. Diameter of the cavity is 6 mm, but in the neighborhood of the aperture for ion extraction the cavity is contracted to 4.5 mm in diameter over the length of 8 mm. The cavity wall near the aperture is shaved down by 1.5 mm. With the above dimension of the cavity, the distance between the repeller and the aperture is 3.5 times as large as the diameter of the cavity, and thus electric field near the repeller and that for ion extraction near the aperture interfere scarcely with each other. Therefore, one can deal with the characteristic of the ion source almost independent of the electric field for ion extraction.

There are two holes of 4 mm in diameter at the head of the cavity body. These holes are useful to lower the gas pressure near the repeller and to decrease the density of positive ions, so that the temperature-rise of the repeller due to ion bombardment is reduced. Without those holes, the quartz insulator is covered soon with wolfram sputtered from the repeller, and becomes a bad insulator. As a result, the intensity of the deflected beam decreases by about one half.

The aperture for ion extraction is of a rectangular shape of 3 mm×3 mm. In the cyclotron of Kyoto University, multipactoring is suppressed by the negative potential applied to dees (called "dee bias"). Ions captured by dees appear as the current increase of the dee bias and cause the load increase of the ac-

celerating RF circuit. The increase of the dee bias current must be maintained below 8 mA in order to operate the cyclotron stably. In the first place, the rectangular aperture for ion extraction of 3 mm wide and of 12 mm long had been tried, and the increase of the dee bias current was above 20 mA. By decreasing the length of rectangular hole to 8 mm and further to 3 mm, the increase of the dee bias current becomes sufficiently small while the intensity of the deflected beam decreases by only 10% from the first case. This is a reason why a 3 mm \times 3 mm hole is used in the present. After long operation the aperture becomes larger owing to evaporation of the edge material by ion bombardment. This evaporation process is especially violent when the magnetic field of the cyclotron is set at the value somewhat lower than that of resonance condition of acceleration. In this case, most of accelerated ions strike the cavity body of the ion source such that it becomes white heat.

The present ion source is made part of wolfram and part of molybdenum, as mentioned above. These materials stand out high temperature, so that the stable operation of the ion source is maintained at higher arc power than 800 watts.

II-2 Power Supply

The power supply for heating the filament is a 3-phase full wave rectifier of maximum dc output power of $6\text{ V} \times 300\text{ A}$, and its circuit is shown in Fig. 2. The accelerating voltage of electron applied between the filament and the canal electrode (called "arc voltage"*) is supplied from a single-phase full wave rectifier as shown in Fig. 3. In order to operate the ion source under some constant condition, the filament current is regulated so as to keep the arc current constant. The circuit of the regulator is shown in Fig. 4. The voltage drop across standard resistor of 0.1 ohm is compared with the reference voltage. The difference of these voltages is amplified with a 3-stage dc amplifier, and is fed to the saturable reactor to regulate the output voltage of the filament power supply. Character-

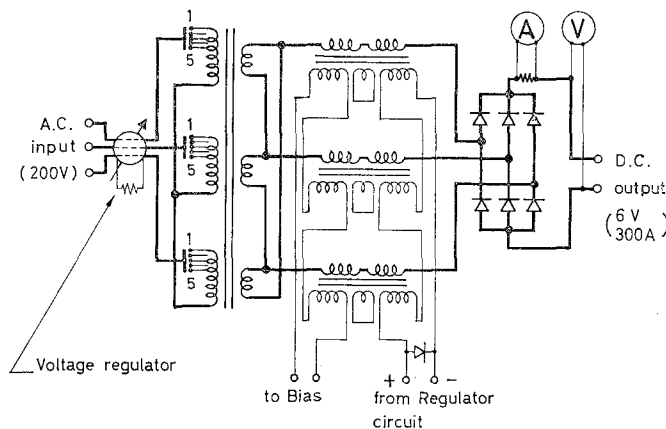


Fig. 2. Power supply for filament current.

* In the present ion source the ionization process is confined in very narrow columnar region. Due to this apparent similarity with the arc discharge, it is customarily called "arc" in many literatures and we also use this name for simplicity and convenience.

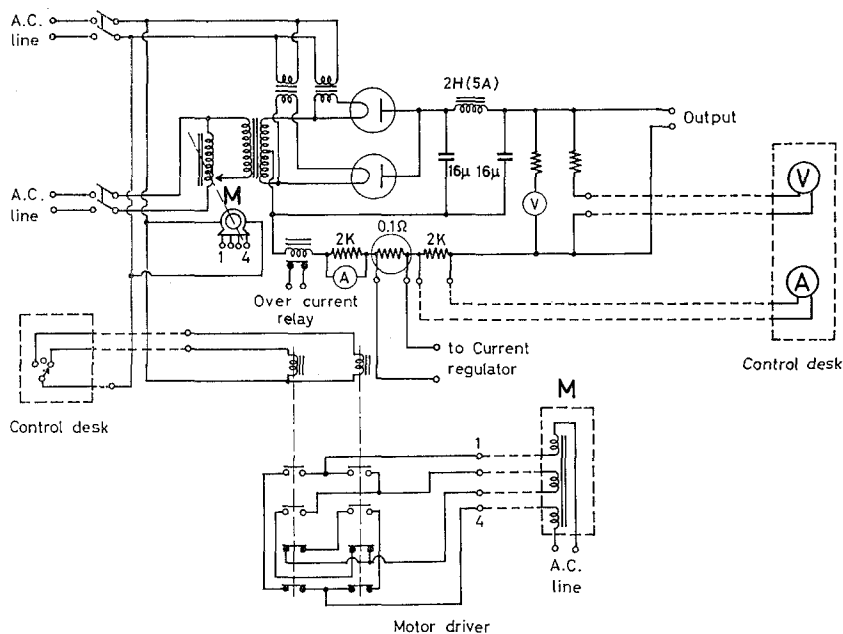


Fig. 3. Power supply for arc voltage.

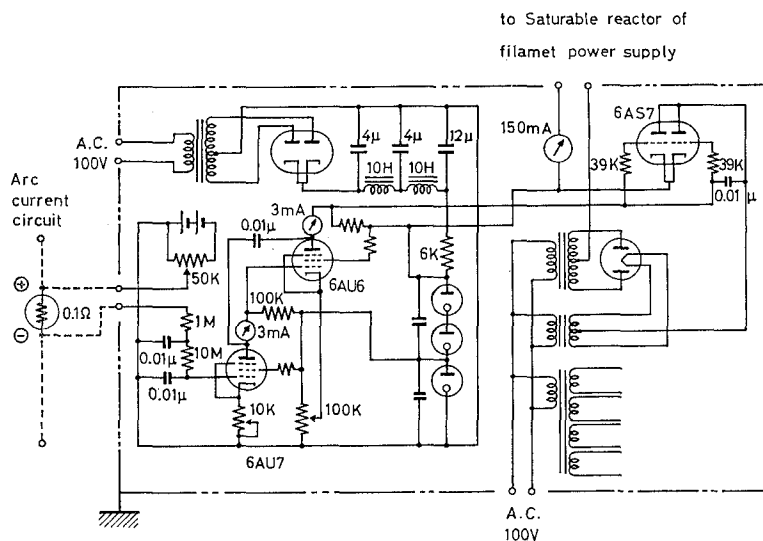


Fig. 4. Regulator circuit for filament current.

istic of this regulator circuit is shown in Fig. 5.

The power supply of arc voltage is placed far apart from the main body of the cyclotron. The earth-side of the arc power supply is connected to the vacuum chamber of the cyclotron.

When the smoothing circuit of the rectifier was insufficient, the modulation of ion beam intensity due to the voltage ripple was observed. Photographs 2 and 3 show such modulation of ion beam intensity observed at the point far apart from

Cyclotron Ion Source

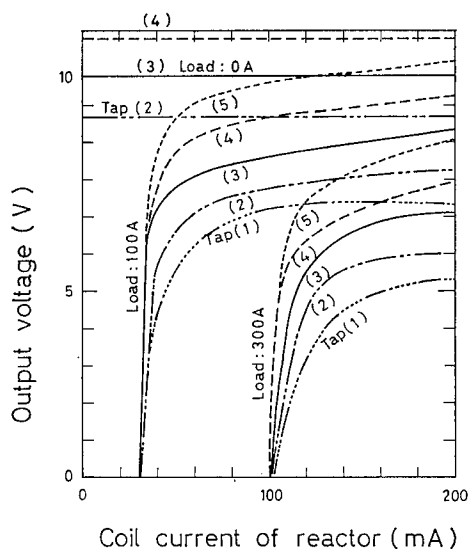


Fig. 5. Characteristics of filament current regulator system. Tap positions 1~5 correspond to those shown in Fig. 2.

the cyclotron. Photograph 2 shows the 120 cps modulated alpha beam intensity due to the ripple of arc voltage at the arc current of 3.5~4.0 A. Photograph 3 shows the 360 cps modulation of H_2^+ ion beam due to the ripple of dc power for the RF oscillator. In this case the ripple of arc voltage is not important because of the small arc current of 1.0 A.

II-3 Gas Supply

Gas is fed into the cavity of the ion source through the filament chamber. The flow rate of gas is regulated by the needle valve shown in Fig. 6. This valve has a gas regulating valve and a gas stop valve separately. The volume of the space between these two valves is made as small as possible (6.4×10^{-2}

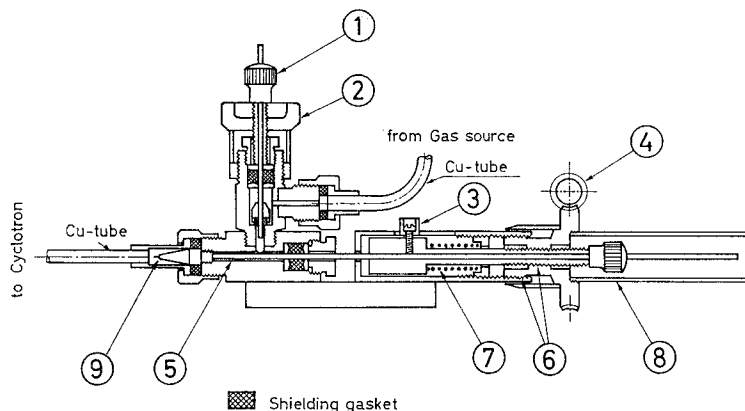


Fig. 6. Needle valve. 1. Shaft chuck, 2. Stop valve, 3. Guide, 4. Worm, 5. Needle valve shaft (1.4 mm in diameter), 6. Differential screw (pitch of 0.115 mm), 7. Spring, 8. Cover, 9. Needle.

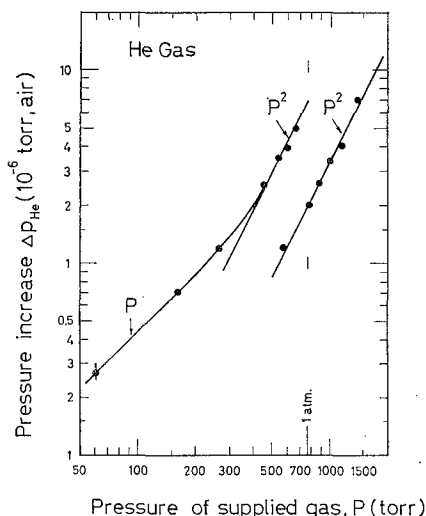


Fig. 7. Characteristics of needle valve. Gas flow rate *vs.* pressure of supplied gas. Pressure increase Δp in the cyclotron due to gas flow is taken as a measure of gas flow rate.

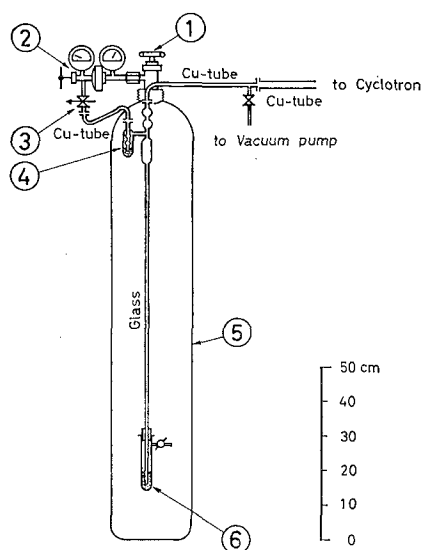


Fig. 8. "Bubble overflow" and "bubble flow meter" equipped to gas-bomb. 1. Main valve, 2. Pressure reducing valve, 3. Slow valve, 4. Bubble flow meter, 5. Gas-bomb, 6. Bubble overflow.

cc), so that this needle valve has the small time constant for the change of gas flow rate and is suitable for checking gas flow. At present, five needle valves are equipped in five gas circuits, respectively. In Fig. 7, the gas flow rates are shown as a function of the pressure of supplied gas before the regulating valve. As the measure of the gas flow rate, the pressure increase Δp in the cyclotron due to gas flow is read with an ionization gauge. Gas flow rate is thought to be proportional to Δp . In this figure, it is apparent that the flow rate increases linearly with the rise of the pressure of supplied gas below 300 torr, and increases with the square of primary pressure above it. This feature corresponds to the fact that gas flow behaves as molecular flow at low pressure and as viscous flow at high pressure. In practice, it is convenient to choose the pressure

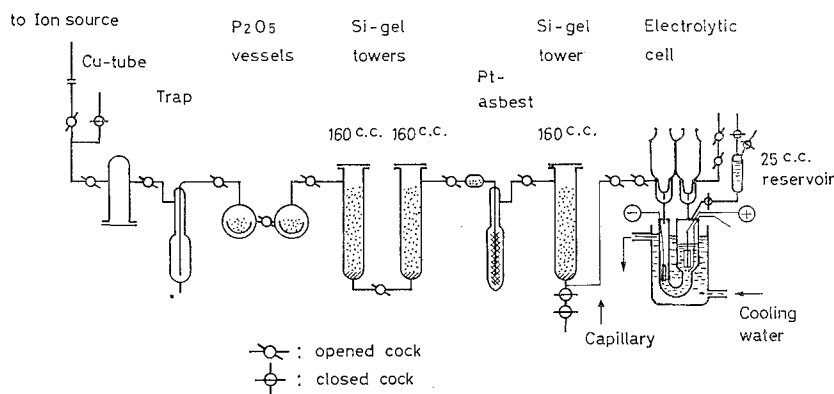


Fig. 9. Assembly of electrolysis and dehydration of H_2 and D_2 gases.

of supplied gas at about 1 atm.. In order to keep the supplied pressure at 1 atm., the "bubble overflow" shown in Fig. 8 is used with gas-bombes of He, N₂ and CO₂. In addition, a "bubble flow meter" is connected in series for monitoring gas flow. Gases of H₂ and D₂ are produced by electrolysis of natural water and heavy water, respectively, and dehydrated by passing through the vessels containing silicagel and P₂O₅. One end of the electrolytic cell is opened in the atmosphere, so that electrolysis proceeds keeping gas pressure at 1 atm.. Gas flow can be monitored by measuring the electrolytic current. This assembly is shown in Fig. 9.

III. PERFORMANCE CHARACTERISTICS

Accelerated ions are extracted from the cyclotron through the deflector and the intensity is measured by the probe electrode placed near the outlet of the deflector. We call this ion beam as "deflected beam".

In Figs. 10a and 10b, the intensity of deflected beam of H₂⁺ ions are shown as a function of the arc voltage and arc current of the ion source. In Figs. 11a, 11b, 12a and 12b, those characteristics for He²⁺ and C²⁺ (CO₂ gas is used) are shown, respectively. From these figures, it is found that the deflected beam intensities of He²⁺ and C²⁺ increase linearly with the arc voltage. For H₂⁺, in contrast to this, the deflected beam intensity saturates at the arc voltage of about 200 volts. The deflected beam intensity of H₂⁺ saturates at the arc current of about 0.5 A. After a few day's operation, this saturation begins at far smaller arc current. For He²⁺, the deflected beam intensity increases linearly with the arc current below about 2.0 A and shows rapid increase above it. For C²⁺, the

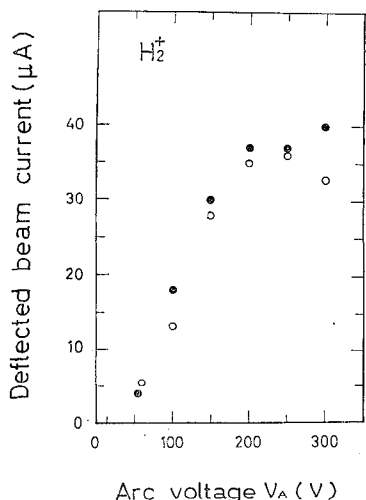


Fig. 10a. Deflected beam current *vs.* arc voltage V_A for H₂⁺.

●: $\Delta p = 6.0 \times 10^{-6}$ torr, ○: $\Delta p = 3.7 \times 10^{-6}$ torr, arc current $I_A = 1.0$ A for both cases.

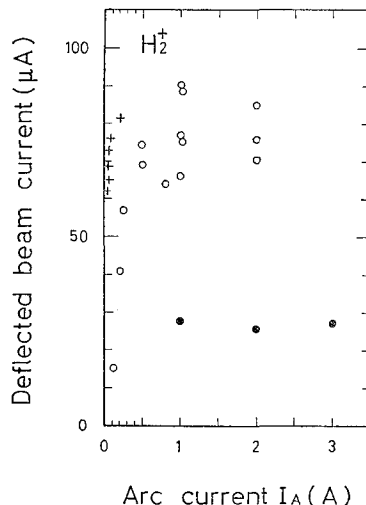


Fig. 10b. Deflected beam current *vs.* arc current I_A for H₂⁺.

●: $V_A = 50$ V, ○: $V_A = 100$ V, +: $V_A = 100$ V (after a few days' operation), $\Delta p = 0.45 \times 10^{-5}$ torr for all cases.

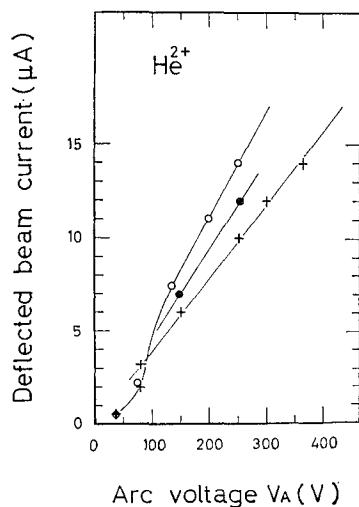


Fig. 11a. Deflected beam current *vs.* arc voltage V_A for He^{2+} .
 ●: $\Delta p = (0.66 \sim 0.58) \times 10^{-5}$ torr,
 ○: $\Delta p = (0.48 \sim 0.44) \times 10^{-5}$ torr,
 +: $\Delta p = (0.35 \sim 0.22) \times 10^{-5}$ torr,
 $I_A = 1.0$ A for all cases.

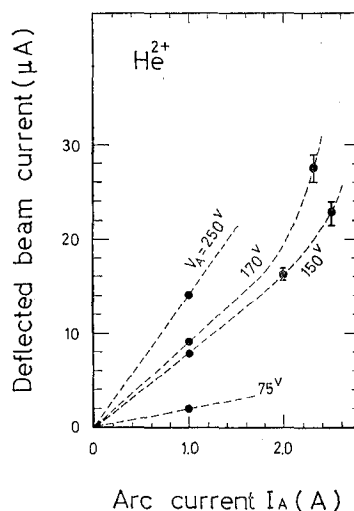


Fig. 11b. Deflected beam current *vs.* arc current I_A for He^{2+} .
 $\Delta p = (0.48 \sim 0.49) \times 10^{-5}$ torr for all cases.

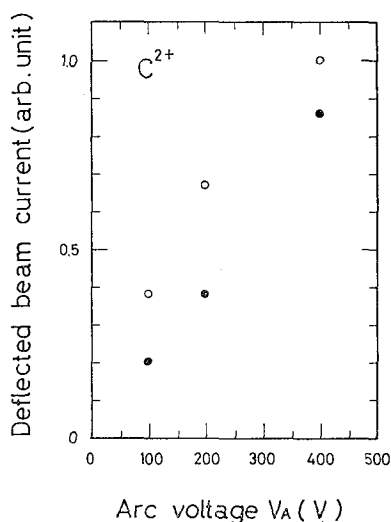


Fig. 12a. Deflected beam current *vs.* arc voltage V_A for C^{2+} .
 ●: $I_A = 0.25$ A, ○: $I_A = 0.5$ A, for both cases,
 $\Delta p = 0.4 \times 10^{-5}$ torr (gas flow rate of ~ 0.3 cc/min).

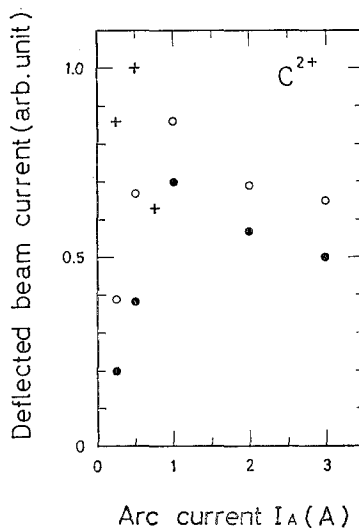


Fig. 12b. Deflected beam current *vs.* arc current I_A for C^{2+} .
 ●: $V_A = 100$ V, ○: $V_A = 200$ V, +: $V_A = 400$ V, for all cases,
 $\Delta p = 0.4 \times 10^{-5}$ torr (gas flow rate of ~ 0.3 cc/min).

deflected beam intensity increases with arc current below about 1 A and decreases above it. Then there are optimum arc powers to obtain large deflected beam intensity for H_2^+ and C^{2+} . On the other hand, the larger arc power is recommended for He^{2+} . The ion source acceptable high arc power is thus favorable. Combinations of the arc current and the arc voltage in usual operation of the ion source are plotted in Fig. 13 for canal electrodes made of graphite and

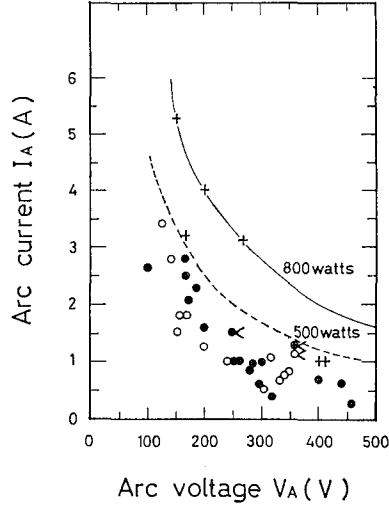


Fig. 13. Combinations of arc current I_A and arc voltage V_A for different canal electrodes.

○: Graphite canal electrode with canal diameter $d=1.5$ mm and separation distance between filament and canal electrode $S=3.0$ mm,

●: Graphite canal electrode, $d=2.0$ mm, $S=1.0$ mm,

+ : Wolfram canal electrode, $d=2.0$ mm, $S=0.75$ mm.

In all cases, He gas is used with $\Delta p=0.4 \times 10^{-5}$ torr. Mark (<) means break down point.

of wolfram. In this figure, the points with the mark (<) correspond to the break-down points that an over-current relay acts shortly due to the arc discharge between the filament and the canal electrode. Break-down points for a wolfram electrode lie at higher arc power (higher than 800 watts) than for a graphite one. The distance between the filament and the canal electrode is desirable to be as small as possible taking into account the starting voltage of self-sustaining gas discharge, but it happened frequently for too small distance that the canal electrode shorted to the filament with small peeled strips of the evaporated wolfram film. The distance of 0.75~1.5 mm is found satisfactory.

In order to operate the cyclotron stably, as described in Section II, it is desirable to reduce ion currents flowing to dees as small as possible. In Figs. 14 and 15, ion currents flowing to dees as a functions of peak dee voltages are shown for H_2^+ and He^{2+} , respectively. Two dees (the dee on the north side is called "N-dee" and that on the south side "S-dee") are grounded through cooling-water circuits, while the dee bias voltage of 870 V is applied to each dee through a current meter. The aperture for ion extraction of the ion source opens to S-

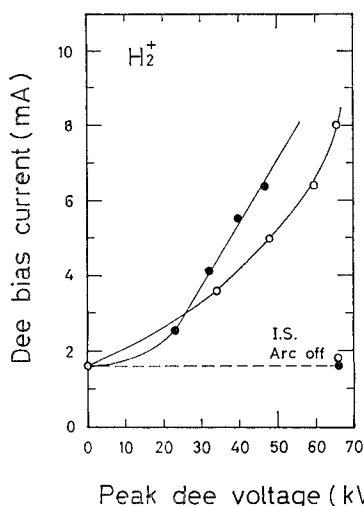


Fig. 14. Dee bias current *vs.* peak dee voltage for H_2^+ .

● : N-dee, ○ : S-dee.

Dee bias voltage = 870 V, $\Delta p = 2.9 \times 10^{-6}$ torr, $V_A = 200$ V, $I_A = 0.8$ A.

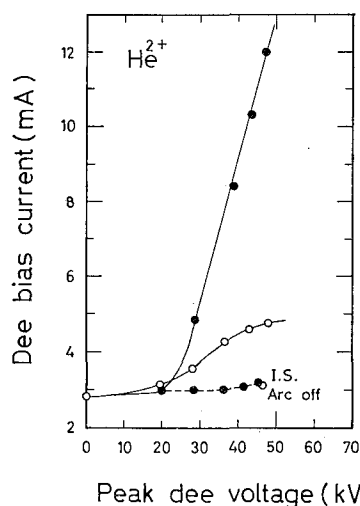


Fig. 15. Dee bias current *vs.* peak dee voltage for He^{2+} .

● : N-dee, ○ : S-dee.

Dee bias voltage = 870 V, $\Delta p = 0.49 \times 10^{-5}$ torr, $V_A = 150$ V, $I_A = 2.5$ A.

dee. When there is no RF voltage, dee bias current is only the current through cooling-water circuit. The bias current read on the current meter increases when the RF voltage is applied. From the fact that the value of dee bias current with RF voltage and zero arc voltage is coincide with that with zero RF voltage and with normal operation of the ion source, it is clear that the increment of the bias current is due to the ion current flowing to the dee. For the increase of the dee bias current above 8 mA, the load increase of the RF resonator causes poor stability of the frequency. Curves of the dee bias current *vs.* peak dee voltage show similar features in N-dee and in S-dee for H_2^+ , but more rapid increase in N-dee than in S-dee for He^{2+} . For He gas, He^+ ions produced in the ion source are much larger in number than He^{2+} ions. Under the condition of the resonant acceleration of He^{2+} , large number of He^+ ions extracted from the ion source are captured by N-dee. This makes the bias current of N-dee much larger than that of S-dee. For H_2 gas, on the other hand, H_2^+ ions and H^+ ions produced in the ion source are comparable in number. Under the resonance condition of H_2^+ the contribution of H^+ ions is not so conspicuous as in the case of He gas.

The relation between the ion current and the rate of gas flow is shown in Fig. 16. For He^{2+} the deflected beam current is measured, while for H_2^+ and H^+ the circulating ion current in the cyclotron is measured by the probe inserted along the center line of dee gap under the respective resonant magnetic fields. The increment of the gas pressure in the cyclotron due to gas flow is used as the measure of the rate of gas flow. Experimental points are too small in number to lead to some definite conclusions, but show the tendency of larger ratio of H^+/H_2^+ for smaller gas flow rate. For He gas, maximum intensity of He^{2+} ions is attained at the increment of gas pressure of about 4×10^{-6} torr (8.0 cc/

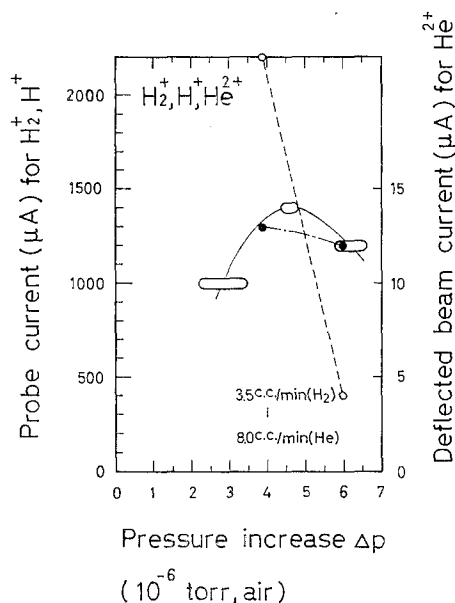


Fig. 16. Ion current *vs.* gas flow rate. Pressure increase Δp in the cyclotron due to gas flow is taken as a measure of gas flow rate. H_2^+ and H^+ ion currents are measured with an inserted probe of which the tip is placed at 400 mm from the center of cyclotron.

○ : H^+ , $V_A=200$ V, $I_A=1$ A,
 ● : H_2^+ , $V_A=200$ V, $I_A=1$ A,
 ○ : He^{2+} , $V_A=250$ V, $I_A=1$ A.

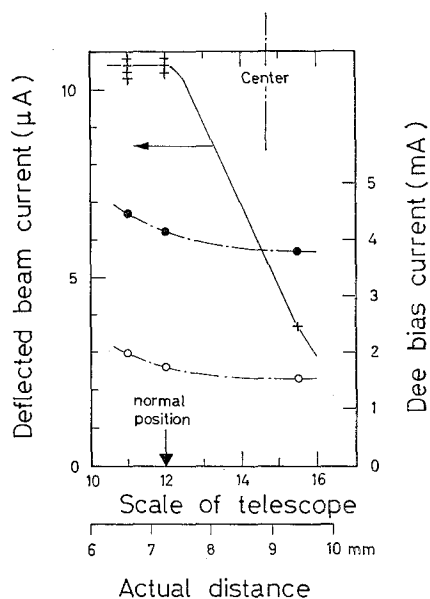


Fig. 17. Dependence of deflected beam current and of dee bias current on ion source position. Position is defined as distance between the body of ion source and the feeler jaw of S-dee.

● : N-dee,
 ○ : S-dee,
 $V_A=200$ V, $I_A=1$ A.

min).

It is found that the deflected beam current increases when the ion source approaches the feeler of S-dee to which the aperture for ion extraction opens. In Fig. 17, the dependence of the dee bias currents and of the deflected beam current on the position of the ion source are shown. The distance between the ion source and the feeler of S-dee is measured on the scale in the telescope from the outside of the cyclotron. On the abscissa of this figure, the reading of the telescope-scale as well as the actual distance are given. The deflected beam current increases with approaching the ion source to S-dee. However, for too small distances only the dee bias current increases without increase of the deflected beam current. In practice, the ratio of distances between the ion source and S-dee and N-dee is chosen to be 12 : 17.

The extraction efficiency of ions from the ion source depends largely on the position of the ionization column which is determined by the position of the canal relative to the axis of the ionization cavity. The deflected beam currents for three different positions shown in Fig. 18 were in the ratio of

$$i_A : i_B : i_C = 1 : 1/2 : 1/3.$$

For position-A, the ionization column stands nearest to the aperture for ion

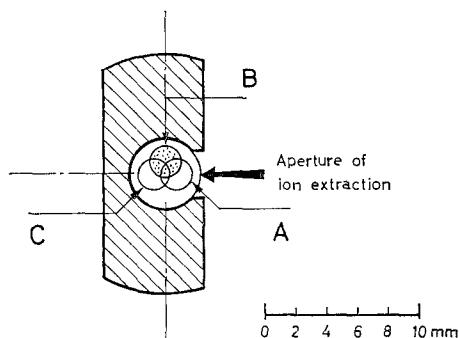


Fig. 18. Three position of canal relative to axis of ionization cavity.
Position A is normal position.

extraction, so that the extracting field is most effective. This position is the normal position of setting.

IV. LIFETIME OF FILAMENT

For practical use, it is very important how long is the lifetime of a filament. It is found that snapping of the filament occurs usually at the position just under the canal (Photo. 4). This means local heating and evaporation of the filament. Positive ions produced near the canal bombard the filament locally just under the canal, so that the temperature at this position of the filament becomes higher than in other position. This local temperature-rise makes the emission of electrons from this part stronger and the density of positive ions near the canal becomes larger. In turn, further local temperature-rise of the filament occurs by the bombardment of dense ions. This part of the filament evaporates and becomes finer and more resistive. Then filament current forces more local temperature-rise and, in turn, much more strong local emission of electrons. As described in Section II-2, the filament current is regulated so as to keep the arc current constant, and then, strong local emission of electrons leads to the suppression of the filament current, and thus primary electrons of arc current are mostly those from the limited part of the filament. In this state, stable operation of the ion source is expected to continue until the filament snaps at this limited position. It is experienced that the ion source becomes the most stable just before the snap of the filament.

From above considerations, the lifetime of the filament can be related quantitatively with the arc current. Taking the arc current to be due to primary electrons emitted from the limited portion of the filament, one can find local temperature of the filament and calculate the rate of evaporation. The curve in Fig. 19 is drawn on the basis of data of thermal electron emission and evaporation from wolfram.⁴⁾ In the abscissa, the arc current as well as the current density of electrons emitted from the area of the filament just under the canal ($\sim 4 \text{ mm}^2$) are shown. The left-side ordinate shows the evaporation rate, and the right-side shows the time required for complete evaporation of the limited part of the filament ($\sim 6 \text{ mm}^3$). The arc current in actual operation is $0.6 \sim$

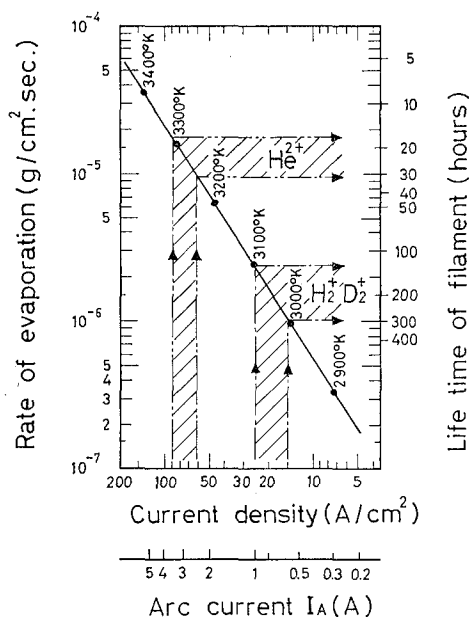


Fig. 19. Lifetime of filament *vs.* arc current I_A . See text for current density.

1.0 A for H_2^+ and D_2^+ and 2.5 to 3.6 A for He^{2+} , and respective life-times of the filament are 130 to 300 h and 15 to 30 h from the figure. These values agree with lifetimes measured for a few hundreds of filaments.

From Fig. 19, it is found that the lifetime of the filament is inversely proportional to the power of 1.7 of the arc current. For example, twice intensity of the arc current reduces the lifetime of the filament by a factor of 3.3.

V. MECHANISM OF ION PRODUCTION

It is very difficult to treat quantitatively the process of ion production in an ion source of any type. In the present ion source also, many unknown factors concerning with the pressure distribution in the cavity, the path of electrons subjected to scatterings in a strong magnetic field, the recombination of ion pairs and so on make it desperate to analyze quantitatively characteristics of the ion source.

The following model for ion production is depicted whenever we are forced to interpret many phenomena qualitatively and to improve the ion source. The verification of this model is to be made from experimental as well as theoretical points in the near future.

Electrons emitted from the filament are accelerated by the voltage between the filament and the canal electrode and enter the cavity. There is no electric field in the cavity, and electrons lose their energies in successive collisions with gas molecules. Strong axial magnetic field confines motions of electrons in narrow columnar region, in which many ion pairs are produced. Ion pairs consist of electrons and atomic or molecular positive ions and their kinetic energies are

so small in average that the ionization power is negligibly small. With diminished energies, primary electrons reach the repeller which is insulated from the cavity wall. At first, the repeller is in equal potential to the cavity wall, so that primary electrons collide with the repeller without any acceleration or deceleration.

When a surface of material is bombarded by electrons, secondary electrons are ejected from the surface, in general. The number of secondary electrons per one incident electron, that is secondary electron emission coefficient δ , is the function of the incident energy such that it increases with the incident energy to some maximum value and thereafter decreases.⁵¹ For wolfram surface, $\delta=1$ at the incident energy of 200 eV, maximum δ is 1.5 at 500 eV and $\delta=1$ at 800 eV. On the other hand, the energy spectrum of secondary electrons has a distribution with maximum intensity at about 2 eV independent of the incident electron energy and with high energy tail. Considering such secondary electron emission, one must distinguish the following two processes according to the energy of electrons colliding with the repeller.

(Process I) When the average colliding energy is above 200 eV, the number of secondary electrons is larger than that of colliding electrons, so that the repeller becomes positive in potential relative to the cavity wall. Succeeding electrons are accelerated by this potential and have larger kinetic energy than preceding ones so as to eject more secondary electrons. Because of low energy of secondary electrons, such charging up process ceases at a positive few volts of the repeller potential. The repeller is heated white in this state by the energy of incident primary electrons, but thermal electron emission is suppressed by positive potential of the repeller. Secondary electrons from the repeller go down in the cavity, but they cannot produce ion pairs owing to their low energies. They repeat elastic scattering with gas molecules until they disappear through recombination with positive ions or they are captured at the bottom of the cavity or at the repeller.

(Process II) When the average colliding energy is below 200 eV, the number of secondary electrons is smaller than that of colliding electrons, so that the repeller is charged up to negative potential. Succeeding electrons are then decelerated by this potential and have smaller kinetic energy than preceding ones, so that δ becomes smaller and the repeller potential becomes more negative. At last, negative potential of the repeller reaches to some value such that all primary electrons are repelled downward in the cavity. While, positive ions produced near the repeller are attracted by the repeller. Positive ions captured by the repeller decrease the negative potential of the repeller to some extent.

The temperature of the repeller becomes very high by the ion bombardment, so that thermal electron emission from the repeller must be taken into account because of the negative potential of the repeller. The secondary electrons due to primary electrons and ions are negligible. In equilibrium, absorption of positive ions and of primary electrons and emission of thermal electrons are to be balanced to give some negative potential of the repeller.

From the following facts, it is concluded that process II takes place in actual

case. Holes at the head of the cavity body play a role to suppress the sputtering of wolfram to the surface of the insulating quartz tube, as described in Section II-1. This fact means that density of ion pairs near the repeller is decreased by the reduction of gas pressure and that the temperature-rise of the repeller is due to ion bombardment. The other fact is that poor insulation of the repeller decreases the intensity of the deflected beam to about one half. Such facts would not be expected if process I occurred.

When the temperature of the repeller is very high, it is expected that the transition of Process II to Process I occurs. In this case, thermal emission of electrons from the repeller is too violent to be compensated by absorption of primary electrons, and the potential of the repeller increases until Process I takes place. In Process I, ionization is made only by primary electrons and not by secondary electrons with low energy. Secondary electrons act only as electron cloud for recombination. Process I, therefore, is unfavorable for operation of the ion source. It is thus necessary to pay attention in cooling the floating electrode for this type of ion source. In the present ion source, such cooling is guaranteed with sufficient surface area of the repeller and two holes at the head of the cavity body. These holes are also used for observation of the temperature-color of the repeller.

ACKNOWLEDGMENTS

The authors would like to thank Prof. Takuji Yanabu for his encouragement and valuable management.

Thanks are also due to Prof. Ryutaro Ishiwari, Prof. Akira Katase and Dr. Hidekuni Takekoshi for the construction of the system for electric power supply.

They are grateful to Dr. Kiyoji Fukunaga, Mr. Noboru Fujiwara and Mr. Masaji Yasue for offering the photographs of the modulation of ion beam intensity.

REFERENCES

- (1) K. Kimura, Y. Uemura, M. Sonoda, S. Shimizu, T. Yanabu, R. Ishiwari, J. Kokame, A. Katase, I. Kumabe, S. Yamashita, H. Takekoshi, K. Miyake, H. Ikegami, and H. Fujita, *Bull. Inst. Chem. Res., Kyoto Univ.*, **39**, 368 (1961).
- (2) F. Fukuzawa, N. Imanishi, M. Sakisaka, K. Yoshida, Y. Uemura, S. Kakigi, and H. Fujita, *Bull. Inst. Chem. Res., Kyoto Univ.*, **45**, 363 (1967).
- (3) R. S. Livingston and R. J. Jones, *Rev. Sci. Instr.*, **25**, 552 (1954).
- (4) "Handbook of Chemistry and Physics", 38th edition (Chemical Rubber Publishing Co.).
- (5) A. von Engel, "Ionized Gases" (Oxford University Press, 1955).